CAAP Quarterly Report

Date of Report: *January 16, 2019*

Contract Number: 693JK31850012CAAP

Prepared for: *USDOT Pipeline and Hazardous Materials Safety Administration (PHMSA)*

Project Title: *Magnet-assisted Fiber Optic Sensing for Internal and External Corrosion-induced Mass losses of Metal Pipelines under Operation Conditions*

Prepared by: *Missouri University of Science and Technology (Missouri S&T)*

Contact Information: *Genda Chen, Ph.D., P.E., F.ASCE, Email: gchen@mst.edu, Phone: (573) 341-4462*

For quarterly period ending: *December 31, 2018*

Business and Activity Section

(a) Generated Commitments – Dr. Genda Chen directed the entire project and coordinated various project activities.

Mr. Liang Fan and Mr. Chuanrui Guo, two Ph.D. candidates in civil engineering at Missouri S&T, were on board since the beginning of this project. They are responsible for the fabrication and characterization test of sensors under Dr. Chen's supervision.

(b) Status Update of Past Quarter Activities – Detailed updates are provided below by task.

Task 1 Optimization of a magnet-assisted hybrid FBG/EFPI sensor enclosed in a plexiglass container for simultaneous measurement of temperature and pipe wall thickness

In-line extrinsic fiber optic interferometer (EFPI) operates based on the reflection of incipient light. In general, an EFPI consists of two parallel reflecting surfaces separated by a cavity with a physical length of L as shown in Figure 1. The reflector can be one end of an optical fiber or a mirror with high reflectivity. In this study, the EFPI is formed by an optical fiber and a gold coated reflective mirror, which is glued to the external surface of a metal pipe to be monitored as shown in Figure 2.

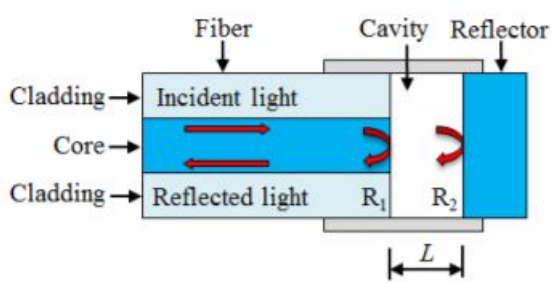

Figure 1. Principle of EFPI

Figure 2. The fabrication and test setup of an EFPI.

Interference occurs between the two coherent light signals that are reflected at two reflecting surfaces, R1 and R2, as shown in Figure 1. The reflection spectrum of the EFPI can be described as a wavelength- dependent intensity modulation of the input light spectrum, which is mainly caused by the optical phase difference between two reflected light beams. The intensity of the interference signal is:

$$P = P_1 + P_2 + 2\sqrt{P_1 P_2}\cos\left(\frac{4\pi n_0 L}{\lambda} + \varphi_0\right) \tag{1}$$

where P1 and P2 are the light intensities reflected from the end-face of the optical fiber and the mirror, respectively; ϕ_0 is the initial phase difference of the interferometer; n_0 is the refractive index of air which is approximately 1, and L is the air cavity length. The two adjacent interference minimums have a phase difference of 2π. That is:

$$\left(\frac{4\pi n_0 L}{\lambda_1} + \varphi_0\right) - \left(\frac{4\pi n_0 L}{\lambda_2} + \varphi_0\right) = 2\pi \tag{2}$$

where λ_1 and λ_2 are the wavelengths of two adjacent valleys in the interference spectrum. Therefore, the cavity length can be calculated as:

$$L = \frac{\lambda_1 \lambda_2}{2(\lambda_1 - \lambda_2)} \tag{3}$$

The cavity length in an EFPI can be calculated from Equation (3). The following shows two test results. In each test, five sets of two adjacent valleys of wavelength are listed and used to calculate the average cavity length.

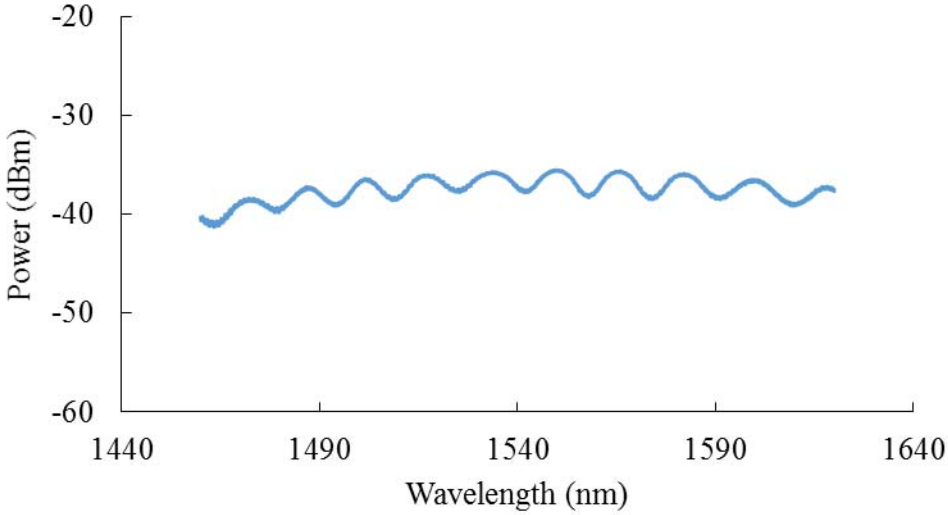

Figure 3. Power spectrum from Test 1.

Table 1. Five sets of two adjacent valleys of wavelength and the calculated cavity length in test 1

λ_1(nm)	1494	1509	1525	1542	1558
λ_2 (nm)	1509	1525	1542	1558	1574
Cavity length (μm)	75.15	71.91	69.16	75.08	76.63

Based on the test results, the average cavity length is 73.59 μm.

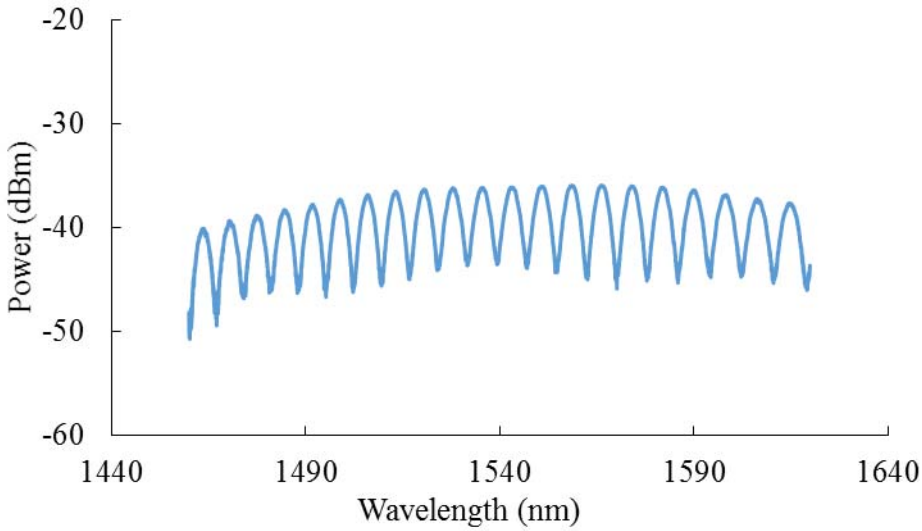

Figure 4. Power spectrum from Test 2.

Table 2. Five sets of two adjacent valleys of wavelength and the calculated cavity length in test 2

λ_1(nm)	1509	1517	1524	1562	1547
λ_2 (nm)	1517	1524	1532	1570	1555
Cavity length (μm)	143.07	165.14	145.92	153.27	150.35

Based on the test results, the average cavity length 151.55 μm.

Task 2 Development and validation of a graphene-based LPFG sensor with Fe-C coating for improved sensitivity in mass loss measurement in varying temperature environment

This task will not start till the 2st quarter in 2019.

Task 3 Integration and field validation of multiple FBG/EFPI and multiplexed LPFG sensors for internal and external corrosion monitoring of a pipeline with temperature compensation.

This task will not start till the 2st quarter in 2020.

(c) **Planned Activities for the Next Quarter -** The following activities in task 1 will be executed during the next reporting quarter.

Task 1 Optimization of a magnet-assisted hybrid FBG/EFPI sensor enclosed in a plexiglass container for simultaneous measurement of temperature and pipe wall thickness

In the next quarter report, the EFPI sensor for internal pipeline corrosion monitoring will be built. The sensor is fabricated in the following steps: (1) the optical fiber passes through the axis of the cylinder permanent magnet and is bonded to the magnet so that they can move together under the magnetic force; (2) the magnet is glued to one end of the plexiglass tube and the other end of the plexiglass will be glued to the rubber pad, which is further glued to the outside surface of steel pipe; (3) the gold coated reflective mirror is glued to the external surface of steel pipe and installed perpendicular to the optic fiber. Once the steel pipe is corroded, the thickness will be reduced and the magnetic force will decrease. The magnet will move away from the steel pipe and increase the cavity length inside the EFPI sensor.

The following four experiments will be conducted. First, the cavity length in the EFPI will be adjusted through a microcalliper to test the sensitivity of an EFPI. The smallest cavity length change needs to be decided to ensure the senor is satisfied for measurement of pipe thickness change. Second, the height of plexiglass needs to be small enough to ensure the magnetic force is strong between magnet and the steel pipe. Third, the magnet size needs to be determined so that the magnetic force is strong but is not too dangerous to operate. Fourth and last, the thickness and size of the rubber pad needs to be determined so that the rubber has elastic deformation under magnetic force.